Hindawi
Discrete Dynamics in Nature and Society
Volume 2020, Article ID 3162170, 10 pages
https://doi.org/10.1155/2020/3162170

Research Article

Sequence of Routes to Chaos in a Lorenz-Type System

Fangyan Yang,[1] Yongming Cao,[2] Lijuan Chen ,[3] and Qingdu Li [2]

[1]*School of Mechanical Engineering, University of Shanghai for Science and Technology, Shanghai 200093, China*
[2]*Chongqing Key Laboratory of Complex Systems and Bionic Control, Chongqing University of Posts and Telecommunications, Chongqing 400065, China*
[3]*School of Mathematical Science, University of Electronic Science and Technology of China, Chengdu Sichuan 611731, China*

Correspondence should be addressed to Lijuan Chen; tangchenlj@163.com

Received 4 September 2019; Accepted 28 October 2019; Published 23 January 2020

Academic Editor: Miguel Ángel López

This paper reports a new bifurcation pattern observed in a Lorenz-type system. The pattern is composed of a main bifurcation route to chaos ($n = 1$) and a sequence of sub-bifurcation routes with $n = 3, 4, 5, \ldots, 14$ isolated sub-branches to chaos. When n is odd, the n isolated sub-branches are from a period-n limit cycle, followed by twin period-n limit cycles via a pitchfork bifurcation, twin chaotic attractors via period-doubling bifurcations, and a symmetric chaotic attractor via boundary crisis. When n is even, the n isolated sub-branches are from twin period-$n/2$ limit cycles, which become twin chaotic attractors via period-doubling bifurcations. The paper also shows that the main route and the sub-routes can coexist peacefully by studying basins of attraction.

1. Introduction

Nonlinear phenomena in physics and engineering are often described by quadratic systems, such as the famous Lorenz system [1], the Nose-Hoover equations [2, 3], the brushless DC motor system [4], the pendulum system [5], etc. A fundamental requirement for such systems is to understand all their behaviors. However, it is a hard task, even for two dimensional (2D) cases (e.g., the Hilbert's sixteenth problem). When the dimension is three or more, the existence of chaos makes it even harder to establish a general theory. Therefore, scientists from various backgrounds devoted themselves to exploiting nonlinear dynamics, especially chaos in Lorenz-type systems, in recent years [6–11].

The most interesting feature of chaos is perhaps that it looks random but simple sequences and patterns are hidden behind. In the Sarkovskii theorem, the Sarkovskii ordering of the natural numbers implies the famous corollary by Li and York: if a continuous map defined on the real line has a period-3 point, then it must have periodic points of every other periods [12]. In the route to chaos, there is usually a sequence of period-doubling (PD) bifurcations as a parameter is adjusted. In Smale's horseshoe [13] or a topological horseshoe [14–16], chaos can be explained by a sequence of operations: squishing, stretching, and folding. Near the quadratic homoclinic tangency, Gavrilov, Silnikov, and Newhouse proved the existence of long period sinks at an infinite sequence of parameter values [17, 18]. For better understanding of the complexity of chaos, whether there are more simple patterns or sequences is always a fundamental question to ask.

In 1992, Petrov et al. found mixed-mode oscillations in a chemical system [19]. They found a pattern composed of a sequence of n isolated sub-branches in a one-parameter bifurcation diagram, where for each $n = 2, 3, 4, \ldots$, the n isolated sub-branches initiate from a period-n limit cycle and lead to chaos via period doubling bifurcations. Recently, similar pattern has also been found in hybrid dynamical system, i.e., the simplest walking model [20, 21]. More recent study suggests that this regular pattern may also exist in the compass-like walking model [22] and the simple walking model with upper body [23]. Although the period of the initial limit cycle increases with step size 1, the pattern is different from the period-adding phenomena reported in [24–26] since there is no parameter overlap between these branches and the period-doubling and period-adding happen in different parameter-changing directions. For this phenomenon, the maximal n found is 7, and the systems are all nonsymmetrical. Therefore, it is interesting to see the situation with a larger n for a symmetrical system.

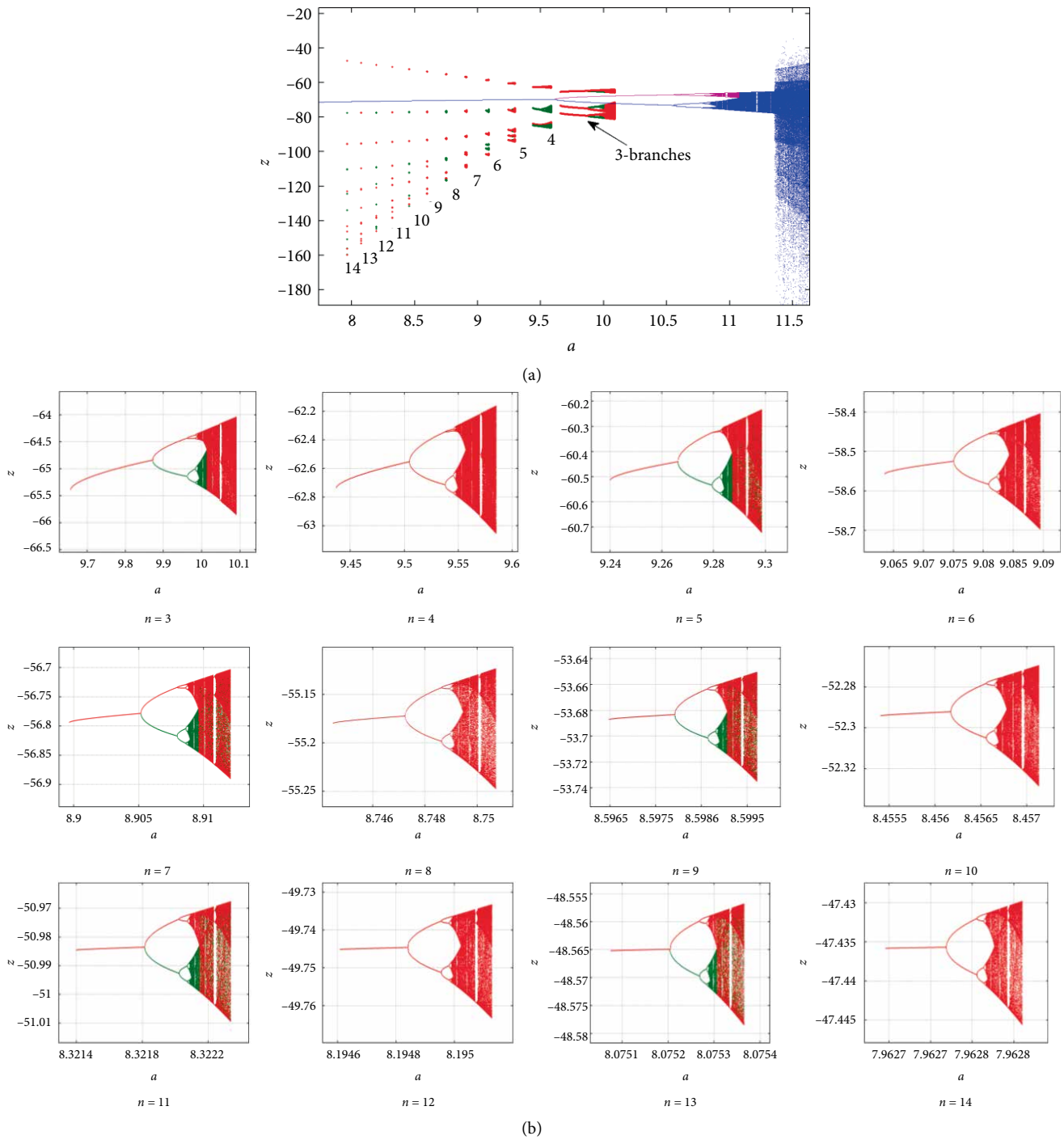

(a)

(b)

Figure 1: Sequence of routes with n sub-branches to chaos.

Therefore, this paper will study a Lorenz-type system and show a sequence sub-branch with n up to 14. When n is odd, the n isolated sub-branches are from a period-n limit cycle, otherwise the n sub-branches are from twin period-$n/2$ limit cycles. Although all these branches lead to chaos as a parameter increases, this pattern is completely different (see Figure 1) from the existing literature, according to the best of the authors' knowledge.

The rest of paper is organized as follows: Section 2 introduces the Lorenz-type system, studies its symmetry, equilibria and their stability, and briefly explores the nonlinear dynamics; Section 3 carries out detailed numerical research on the sequence of bifurcation branches; Section 4 draws the conclusion.

2. The Lorenz Type System

The Lorenz type system is given by following equations:

$$\begin{aligned} \dot{x} &= -ax - by + yz, \\ \dot{y} &= -cx - xz, \\ \dot{z} &= -x^2 + xy - dz, \end{aligned} \tag{1}$$

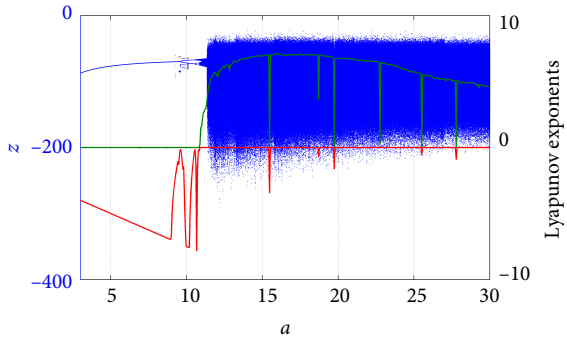

FIGURE 2: The bifurcation diagram and the Lyapunov exponents by varying a.

where x, y and z are the state variables, and a, b, c and d (when $d \neq 0$, this parameter can be eliminated with replacement $x \to d\hat{x}$, $y \to d\hat{y}$, $z \to d\hat{z}$, $a \to \hat{a}d$, $b \to \hat{b}d$, $c \to \hat{c}d$ and $t \to \hat{t}/d$) are positive parameters. Comparing with the famous Lorenz system, although there are some different terms, it has similar reflection symmetry, dissipation, equilibria, and even chaotic attractor. Obviously, system (1) is invariant under the same transformation,

$$(x, y, z) \leftrightarrow (-x, -y, z). \tag{2}$$

Therefore, if $(x(t), y(t), z(t))$ is a solution of (1), then $(-x(t), -y(t), z(t))$ is also a solution. Since the Jacobian matrix of (1) at (x, y, z) is,

$$J = \begin{bmatrix} -a & z-b & y \\ -c-z & 0 & -x \\ y-2x & x & -d \end{bmatrix}. \tag{3}$$

It is easy to see that the system is dissipative because there exists an exponential contraction rate,

$$\nabla V = \frac{\partial \dot{x}}{\partial x} + \frac{\partial \dot{y}}{\partial y} + \frac{\partial \dot{z}}{\partial z} = -(a+d) < 0. \tag{4}$$

Since $\Delta = (cd/(b+c)(a+b+c)) > 0$, system (1) has three equilibria. The first one is the origin O, and the eigenvalues of the Jacobian matrix (3) at O are,

$$\begin{aligned} \lambda_1 &= -\frac{a}{2} + \frac{\sqrt{a^2+4bc}}{2}, \\ \lambda_2 &= -\frac{a}{2} - \frac{\sqrt{a^2+4bc}}{2} \\ \text{and } \lambda_3 &= -d. \end{aligned} \tag{5}$$

Since all parameters are positive, we have $\lambda_1 > 0$, $\lambda_2 < 0$ and $\lambda_3 < 0$, which means that O is unstable. The other two equilibria are,

$$\begin{aligned} O^- &= \left(-(b+c)\sqrt{\Delta},\ a\sqrt{\Delta},\ -c\right) \\ \text{and } O^+ &= \left((b+c)\sqrt{\Delta},\ -a\sqrt{\Delta},\ -c\right), \end{aligned} \tag{6}$$

which are obviously symmetric to each other under transformation (2). When the parameters take the following values,

$$\begin{aligned} a &\in [3,\ 30], \\ b &= 3, \\ c &= 63.5, \\ \text{and } d &= 5. \end{aligned} \tag{7}$$

They are both unstable. For example, when $a = 15$, the eigenvalues at both O^- and O^+ are $\lambda_{1,2} \approx 11.09 \pm 30.58i$, and $\lambda_3 \approx -39.18$.

To explore the nonlinear dynamics of this system, we compute Lyapunov exponents and a bifurcation diagram with the same initial condition (0, 0.01, 0.01) as a varies from 3 to 30. For Lyapunov exponents, we use the QR-based Jacobian method and the final time takes 10,000 to ensure a good accuracy. For the bifurcation diagram, we first take $\Pi = \{(x, y, z) | x = 0 \text{ and } \dot{x} < 0\}$ as a Poincaré cross-section plane, and then define a Poincaré map $h : \Pi \to \Pi$ as follows: For each $\mathbf{x} \triangleq (y, z) \in \Pi$, $h(\mathbf{x})$ is taken to be the first return point in Π under the flow of system (1) with the initial condition $\mathbf{x}$. To exclude transient behaviors of iterating h, we discard the first 1000 points, and then save the following 1000 points.

The numerical results are shown in Figure 2 with double axes where the left axis indicates the bifurcation diagram and the right axis indicates Lyapunov exponents. Since the last Lyapunov exponent is always a large negative number, it is not displayed. Figure 2 suggests that the Lyapunov exponents and the bifurcation diagram match very well and both show rich complex behaviors.

When $3 \leq a < 9.612$, system (1) has a limit cycle with period-1. A typical phase portrait at $a = 5$ is illustrated as the first row in Figure 3 with three different view angles. As a increases from 9.621, there seems a period-doubling route to chaos. A typical chaotic attractor at $a = 11.2$ is shown in the second row in Figure 3, and its three Lyapunov exponents are 2.90, 0.00, and −19.10, respectively. While a keeps increasing, the largest Lyapunov exponent also increases. When $a \approx 11.36$, the chaotic attractor suddenly becomes a large chaotic attractor. A typical large chaotic attractor at $a = 15$ is shown in the last row in Figure 3, and its three Lyapunov exponents are 6.94, 0.00, and −26.94, respectively. When a increases from 15, the largest Lyapunov exponent may jump to zero occasionally, which indicates some periodic windows in the bifurcation diagram.

3. Sequence of Routes to Chaos

If one carefully looks at the bifurcation diagram in Figure 2, two unexpected issues will be found: (1) The period-doubling route seems broken near $a = 10.69$; (2) There are many points located outside of the main bifurcation branch near $a = 10$. The following detailed study will lead us to a sequence of sub-bifurcation routes to chaos, as shown in Figure 1(a).

3.1. The Main Branch B_1 to Chaos from the Period-1 Limit Cycle. For the first issue, we trace the bifurcation diagram by continuation. The results are shown in Figure 4(e) with the left axis, where the bifurcation branches in magenta and blue indicate different attractors. When $a = 9.5$, there is only one limit cycle with period-1, as shown in Figure 4(a). At $a \approx 9.612$, this cycle bifurcates into two different period-1 limit

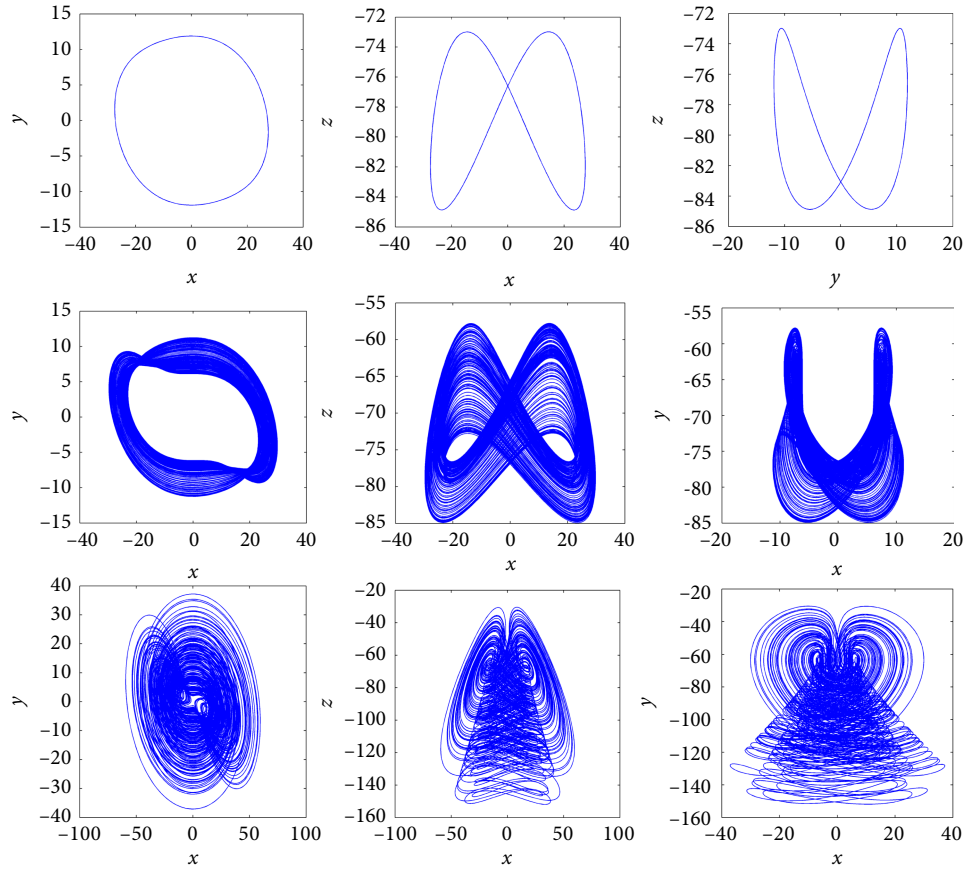

Figure 3: Typical phase portraits at $a = 5$, 11.2 and 15.

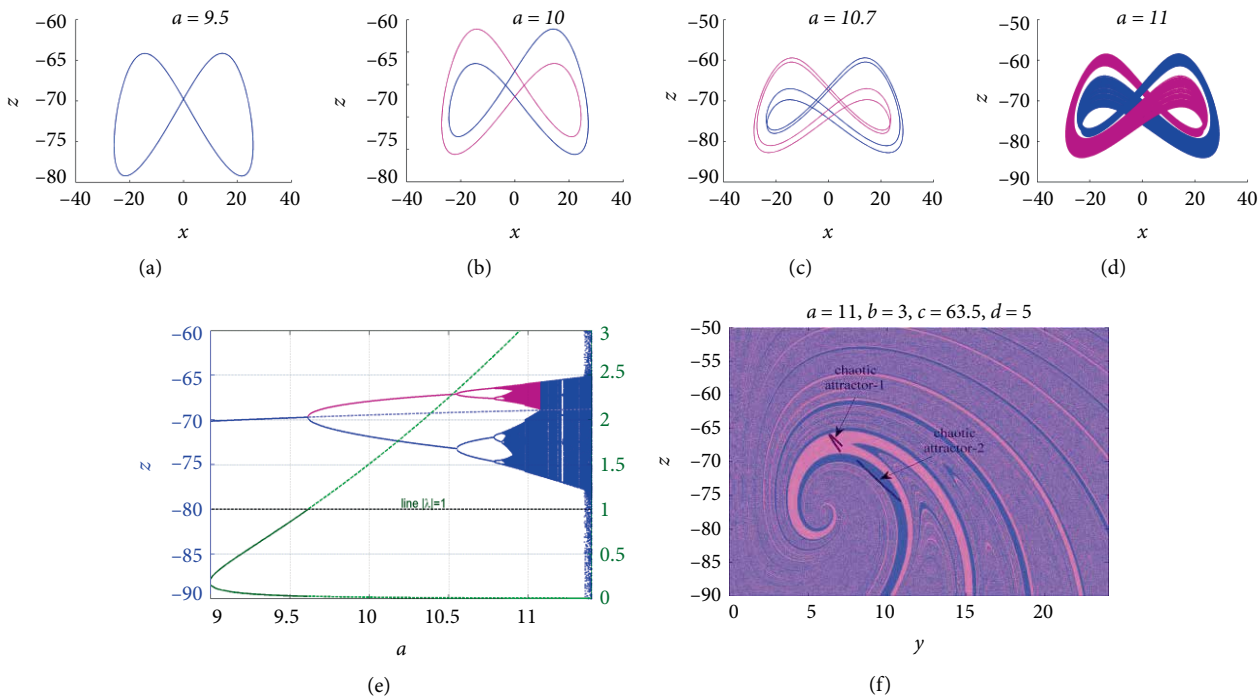

Figure 4: The detailed dynamics and bifurcations of the main branch.

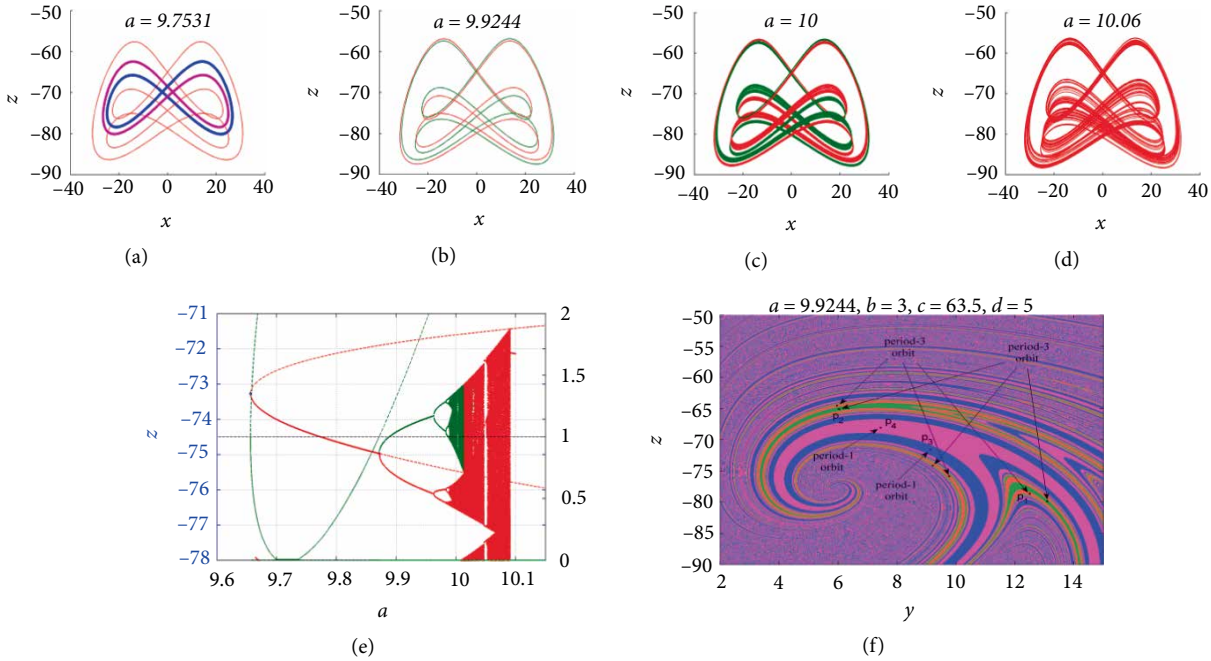

Figure 5: The period-3 limit cycle, its bifurcations and basin of attraction.

cycles. The new-born "twin" limit cycles are shown in Figure 4(b). Here "twin" means that they are the same under the transformation (2). As a increases, each limit cycle becomes a chaotic attractor via a sequence of period-doubling bifurcations. A typical phase portrait of the two chaotic attractors is shown in Figure 4(d). They are also symmetric to each other, and their Lyapunov exponents are 1.65, 0, and −17.65. They can peacefully coexist, and their basins of attraction are shown in Figure 4(f), which suggest that the boundaries are fractal. At last, the twin chaotic attractors merge into one chaotic attractor at $a \approx 11.08$ due to a boundary crisis. The merged attractor at $a = 11.2$ has already been shown in the middle row of Figure 3.

To examine how the original cycle bifurcates into the twin cycles, we compute the eigenvalues of the Jacobian of the Poincaré map h along the period-1 cycle. The eigenvalues are shown in Figure 4(e) with the right axis, where the blue dot line indicates the period-1 cycle after the bifurcation, and the green solid and dot lines indicate the absolute eigenvalues before and after the bifurcation, respectively. Since one eigenvalue crosses the unit circle from inside to outside at 1.0, it belongs to a pitchfork bifurcation, which is introduced by the reflection symmetry of the system.

3.2. Sub-Branches B_3 to Chaos from a Period-3 Limit Cycle. For the second issue, we trace those points out of the main branch via continuation while adjusting a up and down, and find a sequence of sub-bifurcation branches consisted of new attractors, which can peacefully coexist with the attractors in the main branch.

When $9.6568 < a < 10.0903$, although there are a pair of twin chaotic attractors in the main branch, we find three new sub-branches of bifurcation diagrams. One of them is shown in detail with Figure 5(e). It starts with a period-3 limit cycle, which is mirror symmetric under transformation (2). This period-3 cycle can peacefully coexist with the twin period-1 cycles in the main branch, as shown in Figure 5(a) for $a = 9.7531$, where the initial values are (0, 7.7231, −68.5635) and (0, ±12.5342, −78.6258), respectively. Like Figure 4(e), eigenvalues of the period-3 cycle are shown in Figure 5(e), which suggests that it is introduced by a fold bifurcation (also called a saddle-node bifurcation).

When a increases, there is also a pitchfork bifurcation as shown in Figure 5(e). The period-3 cycle bifurcates into a pair of new twin period-3 cycles at $a \approx 9.8702$. A phase portrait of the twin cycles is depicted in Figure 5(b) at $a \approx 9.9244$. Note that the new twin period-3 cycles can also peacefully coexist with the twin period-1 cycles. Their basins of attraction of h are shown in Figure 5(f), where $P_1 \approx (12.5020, -78.6634)$ and $P_2 \approx (6.0350, -65.0803)$ are from the twin period-3 cycles, and $P_3 \approx (9.1301, -71.6131)$ and $P_4 \approx (7.4409, -68.0668)$ are from the twin period-1 cycles. It is clear to see that all basins have fractional structures, and the boundaries are mixed together in many places, where an initial value could be trapped by any attractor.

Like the main bifurcation branch, the twin period-3 cycles also become a pair of twin chaotic attractors via period-doubling bifurcations as a keeps increasing. A typical phase portrait of the twin chaotic attractors are shown in Figure 5(c) at $a = 10$. When $a \approx 10.0145$, the twin chaotic attractors suddenly merge into one chaotic attractor via a boundary crisis, as shown in Figure 5(d) at $a = 10.06$.

3.3. Sub-Branches B_4 to Chaos from a Pair of Twin Period-2 Limit Cycles. When a takes a smaller range, i.e., $9.4370 < a < 9.5852$, although there is a period-1 limit cycle in the main branch, we find four new sub-branches of bifurcations. Unlike the three sub-branches studied above, they are NOT from one limit cycle with period-4 but from a pair of twin limit cycles with period-2. A typical phase portrait of the twin cycles at $a = 9.4741$ is shown in Figure 6(a). And a detailed branch of the bifurcation diagrams is shown in Figure 6(c) with double axes. It is easy to see that

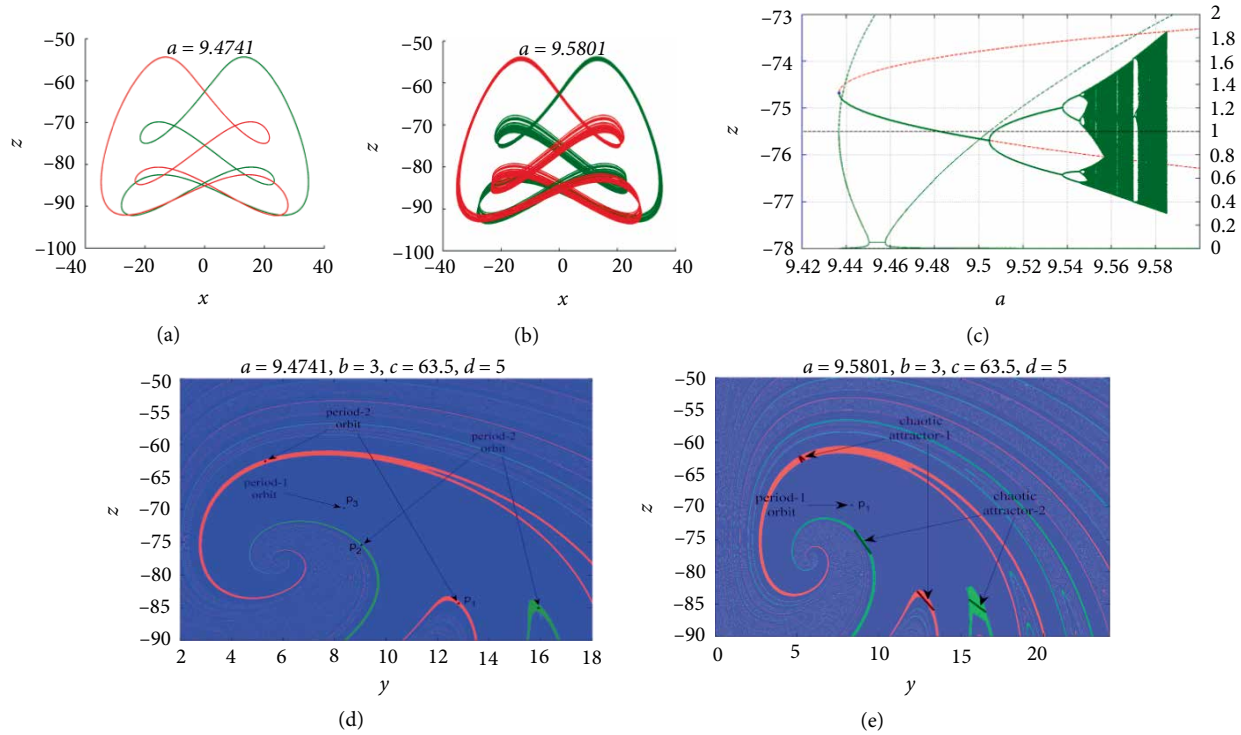

Figure 6: The period-2 limit cycle, its bifurcations and basin of attraction.

the twin limit cycles are also introduced by a fold bifurcation. The basins of attraction are shown in Figure 6(d), where $P_1 \approx (12.8113, -84.3293)$ and $P_2 = (9.0434, -75.4186)$ are from the twin cycles with period-2, and $P_3 = (8.3636, -69.7783)$ is from the main cycle with period-1. Obviously, the three limit cycles can coexist peacefully, and their basins have fractional structures too. When a keeps increasing from 9.4741, the twin period-2 cycles become a pair of twin chaotic attractors via period-doubling bifurcations. A phase portrait of the twin chaotic attractors at $a = 9.5801$ are shown in Figure 6(b), where the initial values are $(0, \pm 12.9744, -84.9422)$. And they have similar basins shown in Figure 6(e).

3.4. Sub-Branches B_5 to Chaos from a Period-5 Limit Cycle. When a takes another smaller range, i.e., $9.2401 < a < 9.2985$, we find five sub-branches of bifurcations outside the main branch. Since five is an odd number like three, the bifurcation phenomenon is similar to the diagram from the limit cycles with period-3, as shown in Figure 7. First, there is a limit cycle (Figure 7(a)) with period-5, which is also introduced by a fold bifurcation (Figure 7(e)), then this cycle bifurcates into a pair of twin limit cycles (Figure 7(b)) with period-5 via a pitchfork bifurcation, after that they become a pair of twin chaotic attractors (Figure 7(c)) via period-doubling bifurcation, at last the twin attractors merge into one larger chaotic attractor (Figure 7(d)).

3.5. Sub-Branches B_6 to Chaos from a Pair of Twin Period-3 Limit Cycles. When a keeps taking a smaller range, i.e., $9.0636 < a < 9.0895$, we find six new sub-branches of bifurcations. Since six is an even number like four, the bifurcation phenomenon is similar to the four sub-branches from the twin limit cycles with period-2, as shown in Figure 8. First, there are a pair of twin limit cycles with period-3 (Figure 8(a)), which are also introduced by a fold bifurcation (Figure 8(c)), and then the twin cycles become a pair of twin chaotic attractors (Figure 8(b)) via period-doubling bifurcations.

3.6. Sequence of Routes to Chaos with More Sub-Branches. According to the above observation, we have a sequence of sub-branches B_n, $n = 3, 4, 5, 6$, which can peacefully coexist with the main branch B_1. When the integer n is odd, e.g., 1, 3, 5, the n sub-branches start with a limit cycle with period-n; otherwise, they start with a pair of twin limit cycles with period-$n/2$. This reminds us of the sequence of bifurcations found in the simplest passive walking model [19], where for each $n \in \{3, 4, 5, 6, 7\}$, there are n sub-branches of period-doubling bifurcations from the period-n gait, and they all can coexist peacefully with the main period-doubling branch from period-1.

Although the bifurcation pattern here is more complex than [19], the sequence is regular enough to predict more sub-branches if they exist. Inspired by Feigenbaum constants, we suppose the following ratio tends to a limit, i.e.,

$$\lim_{n\to\infty} \frac{r_n - r_{n-1}}{r_{n-1} - r_{n-2}} = \eta, \tag{8}$$

where r_n represent the first bifurcation point in B_n. If n is odd, r_n is a pitchfork bifurcation point, otherwise a period doubling bifurcation. Then we predict an approximate value of the next bifurcation point by,

$$r_{n+1} \approx r_n + \frac{(r_n - r_{n-1})^2}{r_{n-1} - r_{n-2}}. \tag{9}$$

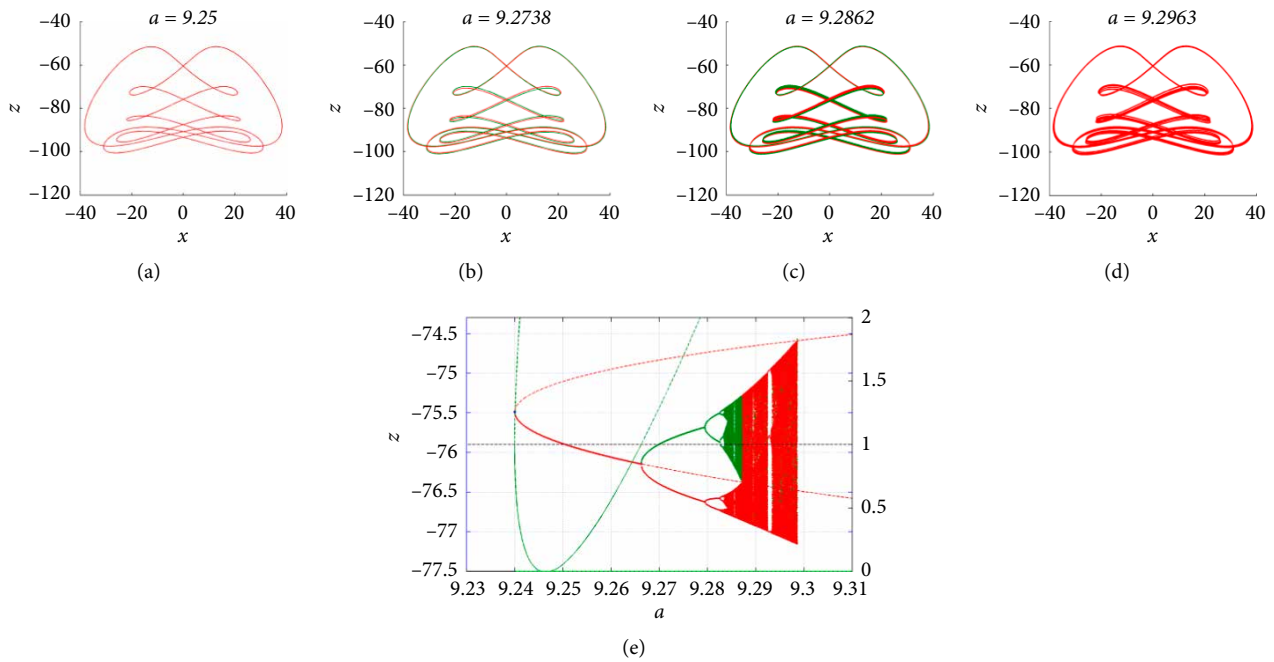

Figure 7: Limit cycle with period-5 and its bifurcation.

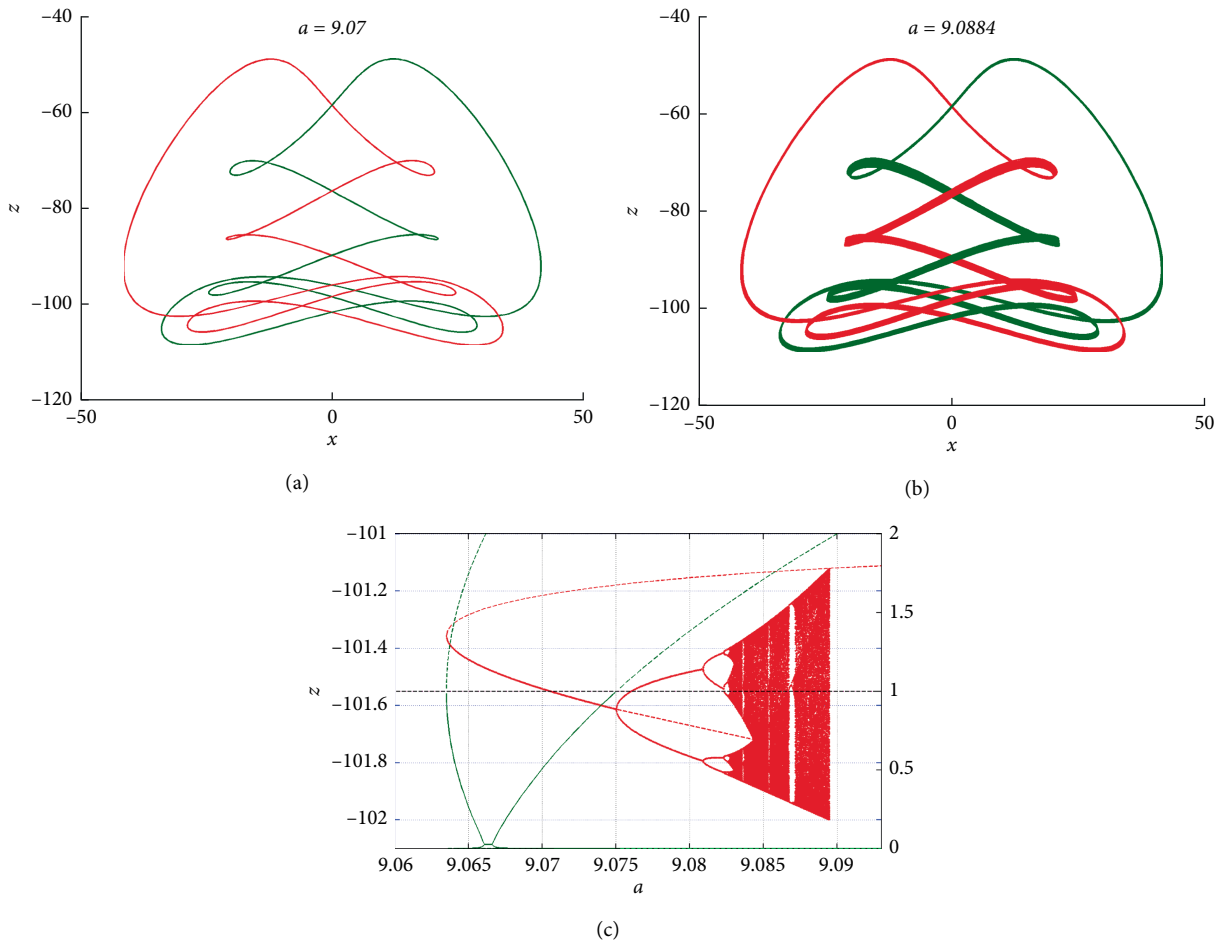

Figure 8: Limit cycle with period-6 and its bifurcations.

Table 1: Sequence of bifurcation points.

n	$\mathbf{x}_n$	a_n	s_n	r_n	$\frac{r_n - r_{n-1}}{r_{n-1} - r_{n-2}}$	$\frac{r_n - s_n}{r_{n-1} - s_{n-1}}$
3	(12.6421, −78.8718)	9.8005	9.655842	9.871091	—	—
4	(12.7825, −84.2335)	9.4646	9.436742	9.504714	—	3.1699
5	(12.5709, −87.4911)	9.2498	9.239972	9.266180	1.5359	2.5995
6	(8.4696, −76.3535)	9.0699	9.063520	9.075047	1.2481	2.2701
7	(8.2565, −76.6158)	8.9023	8.899685	8.905179	1.1246	2.0952
8	(11.7836, −92.3385)	8.7460	8.744490	8.747220	1.0754	2.0000
9	(7.9555, −77.0160)	8.5972	8.596478	8.597911	1.0577	1.9064
10	(11.3884, −93.8690)	8.4558	8.455405	8.456170	1.0533	1.8867
11	(2.1312, −50.9839)	8.3216	8.321398	8.321815	1.0551	1.8201
12	(1.8821, −49.7448)	8.1947	8.194608	8.194839	1.0581	1.8052
13	(1.6619, −48.5650)	8.0751	8.0750751	8.0752041	1.0614	1.7907
14	(13.6614 , −110.2840)	7.9627	7.9626959	7.9627687	1.0640	1.7917

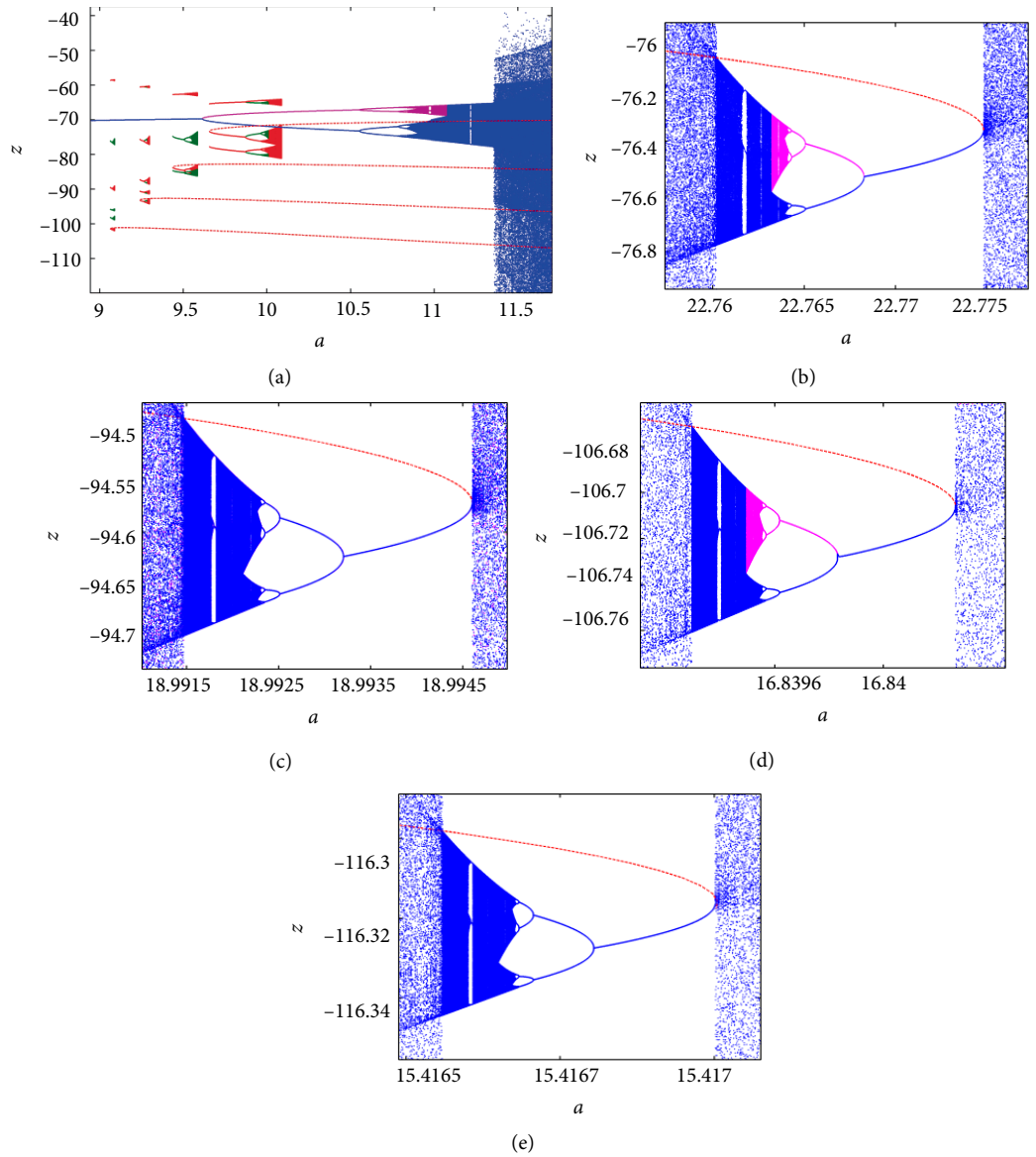

Figure 9: Connections between the sub-branches and the periodic windows.

By searching basins of attraction near this predicted point with the heterogeneous algorithm accelerated by GPU computing proposed in [18], many new sub-branches are found, as shown in Figure 1(a), which successfully extend the sequence up to 14. As listed in Table 1, for the n sub-branches B_n, $\mathbf{x}_n$ indicates an approximate point of the new limit cycle at $a = a_n$, which is induced by a fold bifurcation at $a = s_n$.

The detailed bifurcations are shown in Figure 1(b), which all follows the known pattern: When n is odd, like the branch-3 shown in Figure 5, the n sub-branches first start with a period-n limit cycle introduced by a fold bifurcation, then bifurcate into a pair of twin limit cycles with the same period, after that the twin cycles become a pair of twin chaotic attractors via period doubling bifurcations, at last the twin chaotic attractors merge into one larger chaotic attractor. When n is even, like the branch-4 shown in Figure 6, the n sub-branches start with a pair of twin limit cycles with period-$n/2$, which are also introduced by a fold bifurcation, then they become a chaotic attractor via period-doubling bifurcations.

When n get lager, the parameter range becomes smaller. For the n sub-branches in B_n, the parameter range of the initial limit cycles is $r_n - s_n$. The following range ratio

$$\frac{r_n - s_n}{r_{n-1} - s_{n-1}}, \tag{10}$$

is listed in Table 1. It seems to have a limit under a small error, which should be close to 1.79. This evidence suggests that the parameter range will get smaller very quickly as n grows. Due to unavoidable numerical errors and time-consuming computing, it becomes extremely hard to find new sub-branches with $n \geq 15$.

3.7. Connections with Periodic Windows of the Main Branch. The sequence of the sub-branches come from a sequence of the initial limit cycles with the following period,

$$3, 2, 5, 3, 7, 4, 9, 5, 11, 6, 13, 7, \ldots \tag{11}$$

This sequence is different from the Sarkovskii's ordering. And it is also different from the period-adding phenomenon reported in the existing literature, according to the best of the authors' knowledge. Therefore, it is significant to see where the limit cycles come from.

Note that a period-n cycle of h is a fixed point of h^n. According to degree theory, as the parameter changes, the only possibilities for this fix point are: (a) coming/leaving through the boundary of the (y, z) domain, (b) being born (splitting)/disappearing (merging) in pairs. Therefore, we can track the limit cycles, with numerical continuation algorithms, back before the fold bifurcation.

The results are shown in Figure 9(a). It is interesting to see that all the cycles turn back to the region of chaos, which implies that the cycles might be born in the chaotic attractor. However, when we track the cycles with very small step size, it is surprising to see that they connect with some small periodic windows (see Figure 2) in the main bifurcation diagram. For example, after two-fold bifurcations, the period-3 cycle connects with three sub-branches in a period-3 windows. A detailed bifurcation diagram of one branch is shown in Figure 9(b), it looks like the reverse of the branch in Figure 4(e). Figure 9(c) also shows such a connection for $n = 5$. When n is an even number, the situation is similar. For example, the twin period-$n/2$ cycles with $n = 4$ or $n = 6$ are also a periodic window after two-fold bifurcations. The window also contains a pair of twin limit cycles with period-$n/2$, which bifurcate into a pair of twin chaotic attractors via period-doubling bifurcations, as shown in Figure 9(e).

The above evidence suggests that each branch in our sequence on the left could connect with a branch in a periodic window on the right. Such phenomenon is much different from the phenomenon reported in [19], where the cycles look passing through the main chaotic attractor bifurcated from the period-1 limit cycle.

4. Conclusions

We have studied a Lorenz-type system and revealed a sequence of route to chaos in the following new pattern. For an odd number $n = 3, 5, \ldots, 13$, there are n isolated sub-bifurcation branches started with a period-n limit cycle and followed by twin period-n limit cycles via a pitchfork bifurcation, twin chaotic attractors via a sequence of period-doubling bifurcations and a symmetric chaotic attractor via boundary crisis. For even number $n = 4, 6, \ldots, 14$, there are n sub-branches started with a period-$n/2$ limit cycle, which becomes twin chaotic attractor via period-doubling bifurcations.

In the above pattern, many chaotic attractors are born from limit cycles with high periods. This is much different from most existing results where there is just one chaotic attractor from a period-1 limit cycle. Since the sub-branches with $n \geq 3$ not only coexist with the main branch with $n = 1$, but also connect with its periodic windows via two-fold bifurcations, the pattern revealed in this paper is also different from the period-adding phenomena. In comparison with the phenomenon in the walking models and the chemical system, the sequence here is much longer [21], which is more helpful for further study. In addition, since all equilibria are unstable for the given parameter in (3), we only observed self-excited attractors. Basin of attraction shows that there should be no hidden attractor like the other Lorenz-like system studied in [27, 28].

We hope the studies carried out in the present paper may bring a new insight into the mechanism of chaos and coexisting attractors. For this purpose, it will also be interesting to find this pattern in real physical systems or simple 2D maps.

Data Availability

The data used to support the findings of this study are available from the corresponding author upon request.

Conflicts of Interest

The authors declare no conflict of interest.

Authors' Contributions

Conceptualization, F. Y., Y. C. and L. C.; software, Y. C.; writing—original draft preparation, F. Y.; writing—review and editing, L. C.; supervision, L. C. and Q. L.; funding acquisition, Q. L.

Acknowledgments

This work was funded by the German Research Foundation and National Natural Science Foundation of China, in project Crossmodal Learning under contract Sonderforschungsbereich Transregio 169, the Hamburg Landesforschungsforderungsprojekt Cross and National Natural Science Foundation of China (61773083, 61501073, 61533006).

References

[1] E. N. Lorenz, "Deterministic nonperiodic flow," *Journal of the Atmospheric Sciences*, vol. 20, pp. 130–141, 1963.

[2] S. Nosé, "A unified formulation of the constant temperature molecular dynamics methods," *The Journal of Chemical Physics*, vol. 81, no. 1, pp. 511–519, 1984.

[3] W. G. Hoover, "Canonical dynamics: equilibrium phase-space distributions," *Physical Review A*, vol. 31, p. 1695, 1985.

[4] N. Hemati, "Strange attractors in brushless DC motors," *IEEE Transactions on Circuits and Systems I: Fundamental Theory and Applications*, vol. 41, pp. 40–45, 1994.

[5] A. Shvets and A. Makaseyev, "Deterministic chaos in pendulum systems with delay," *Applied Mathematics and Nonlinear Sciences*, vol. 4, no. 1, pp. 1–8, 2019.

[6] G. Leonov and N. Kuznetsov, "On differences and similarities in the analysis of Lorenz, Chen, and Lu systems," *Applied Mathematics and Computation*, vol. 256, pp. 334–343, 2015.

[7] J. C. Sprott, X. Wang, and G. Chen, "Coexistence of point, periodic and strange attractors," *International Journal of Bifurcation and Chaos*, vol. 23, p. 1350093, 2013.

[8] P. Zhou and F. Yang, "Hyperchaos, chaos, and horseshoe in a 4D nonlinear system with an infinite number of equilibrium points," *Nonlinear Dynamics*, vol. 76, pp. 473–480, 2014.

[9] B. Xu, G. Wang, H. H. C. Iu, S. Yu, and F. Yuan, "A memristor-meminductor-based chaotic system with abundant dynamical behaviors," *Nonlinear Dynamics*, vol. 96, no. 1, pp. 765–788, 2019.

[10] Z. Galias, "Numerical study of multiple attractors in the parallel inductor capacitor memristor circuit," *International Journal of Bifurcation and Chaos*, vol. 27, no. 11, p. 1730036, 2017.

[11] S. S. Hassan, M. P. Reddy, and R. K. Rout, "Dynamics of the modified n-degree Lorenz system," *Applied Mathematics and Nonlinear Sciences*, vol. 4, no. 2, pp. 315–330, 2019.

[12] T. Y. Li and J. A. Yorke, "Period three implies chaos," *American Mathematical Monthly*, pp. 985–992, 1975.

[13] S. Smale, "Differentiable dynamical systems," *Bulletin of the American Mathematical Society*, vol. 73, pp. 747–817, 1967.

[14] X. S. Yang, "Topological horseshoes and computer assisted verification of chaotic dynamics," *International Journal of Bifurcation and Chaos*, vol. 19, pp. 1127–1145, 2009.

[15] Q. D. Li and X. S. Yang, "A simple method for finding topological horseshoes," *International Journal of Bifurcation and Chaos*, vol. 20, pp. 467–478, 2010.

[16] J. Kennedy and J. Yorke, "Topological horseshoes," *Transactions of the American Mathematical Society*, vol. 353, pp. 2513–2530, 2001.

[17] N. Gavrilov and L. Šil'nikov, "On three-dimensional dynamical systems close to systems with a structurally unstable homoclinic curve. II," *Sbornik: Mathematics*, vol. 19, pp. 139–156, 1973.

[18] S. E. Newhouse, "Diffeomorphisms with infinitely many sinks," *Topology*, vol. 13, pp. 9–18, 1974.

[19] V. Petrov, S. K. Scott, and K. Showalter, "Mixed-mode oscillations in chemical systems," *The Journal of Chemical Physics*, vol. 97, pp. 6191–6198, 1992.

[20] Q. Li, H. Zhou, and X. S. Yang, "A study of basin of attraction of the simplest walking model based on heterogeneous computation," *Acta Physica Sinica*, vol. 61, p. 040503, 2012.

[21] Q. Li, S. Tang, and X. S. Yang, "New bifurcations in the simplest passive walking model," *Chaos: An Interdisciplinary Journal of Nonlinear Science*, vol. 23, p. 043110, 2013.

[22] H. Gritli, N. Khraief, and S. Belghith, "Period-three route to chaos induced by a cyclic-fold bifurcation in passive dynamic walking of a compass-gait biped robot," *Communications in Nonlinear Science and Numerical Simulation*, vol. 17, pp. 4356–4372, 2012.

[23] Q. Li, J. Guo, and X. S. Yang, "Bifurcation and chaos in the simple passive dynamic walking model with upper body," *Chaos: An Interdisciplinary Journal of Nonlinear Science*, vol. 24, p. 033114, 2014.

[24] V. S. Piassi, A. Tufaile, and J. C. Sartorelli, "Period-adding bifurcations and chaos in a bubble column," *Chaos: An Interdisciplinary Journal of Nonlinear Science*, vol. 14, pp. 477–486, 2004.

[25] Y. Yang, X. Liao, and T. Dong, "Period-adding bifurcation and chaos in a hybrid Hindmarsh-Rose model," *Neural Networks*, vol. 105, pp. 26–35, 2018.

[26] Y. Li and H. Gu, "The distinct stochastic and deterministic dynamics between period-adding and period-doubling bifurcations of neural bursting patterns," *Nonlinear Dynamics*, vol. 87, no. 4, pp. 2541–2562, 2017.

[27] G. A. Leonov and N. V. Kuznetsov, "Hidden attractors in dynamical systems. From hidden oscillations in Hilbert-Kolmogorov, Aizerman, and Kalman problems to hidden chaotic attractor in Chua circuits," *International Journal of Bifurcation and Chaos*, vol. 23, p. 1330002, 2013.

[28] G. A. Leonov, N. V. Kuznetsov, and T. N. Mokaev, "Self-excited and hidden attractors in a Lorenz-like system describing convective fluid motion," *European Physical Journal Special Topics*, vol. 224, pp. 1421–1458, 2015.